ASSESSMENT OF CMIP6 MULTI-MODEL SIMULATION OF SUBTROPICAL HIGH IN THE NORTHWESTERN PACIFIC OCEAN IN SUMMER

YANG, C. Z.[1] – LI, X. J.[1*] – OUYANG, L.[2]

[1]*Civil Aviation Flight University of China, Chengdu 641419, Sichuan, China*

[2]*Ganzhou Meteorological Bureau, Ganzhou 341000, Jiangxi, China*

**Corresponding author*
e-mail: lxjlucky@126.com

(Received 8th Apr 2025; accepted 11th Jun 2025)

Abstract. This study aims to systematically evaluate the performance of thirteen Coupled Model Intercomparison Project Phase 6 (CMIP6) models in simulating the summertime Northwestern Pacific Subtropical High (NWPSH), with an emphasis on assessing their spatial patterns, climatological characteristics, and long-term trends. Results indicate that certain the CMIP6 models exhibit systematic biases in simulating the 500-hPa geopotential height over the Northwestern Pacific during summer, while performing better in capturing both the interannual variability and spatial amplitude modulation of the geopotential height field. By correcting these systematic biases using NCEP/NCAR observational data, the accuracy of simulations is significantly improved, particularly in depicting the NWPSH indexes and its spatial shape. Quantitative assessments identify EC-Earth3, EC-Earth3-Veg, BCC-ESM1, and MRI-ESM2-0 as superior in reproducing the NWPSH index. Further analysis using Shared Socioeconomic Pathways scenarios (SSPs) reveals distinct future trajectories for NWPSH intensity and spatial position, highlighting the importance of robust model selection for reliable future climate projections in East Asia. Overall, the findings of this study provide essential guidance for selecting and applying the CMIP6 models to improve the accuracy of regional climate change attribution analyses and future climate projections.
Keywords: *multi-model ensemble, indexes evaluation, shared socioeconomic pathways, climatology correction, 500-hPa geopotential height*

Introduction

The Northwestern Pacific Subtropical High (NWPSH) is one of the most important atmospheric circulation systems influencing climate and weather patterns in China and East Asia.

As China is adjacent to the Pacific Ocean and has one of the longest coastlines, its unique geographic location makes the size and location of the NWPSH critically important in shaping China’s climate. The NWPSH determines the distribution of rainbands and the timing of the rainy season in China (Chang et al., 2000; Zhou and Yu, 2005). The inter-decadal changes of the NWPSH have a significant impact on summer precipitation in East Asia (Tao, 1987).

Changes in the intensity and position of the NWPSH can trigger severe climatic extremes, such as widespread flooding and prolonged droughts, notably affecting the middle and lower reaches of the Yangtze River basin (Guan et al., 2019; Jing, 2014; Yang et al., 2011; Wang and Wu, 2024). The inter-decadal changes of circulation factors such as the NWPSH provide a basis for the redistribution of drought and flood conditions in China through changes in climate patterns (Capotondi et al., 2023). The characteristics of the NWPSH’s various elements remain a key issue worth analyzing and exploring, as

http://www.aloki.hu ● ISSN 1589 1623 (Print) ● ISSN 1785 0037 (Online)
DOI: http://dx.doi.org/10.15666/aeer/2304_78997919

they are crucial for understanding regional variations in rainy seasons, changes in intensity, and the mechanisms driving precipitation during the flood season in China (Tao, 2006).

Currently, climate models represent the primary tool for studying and predicting climate changes. Previous assessments of climate system models, particularly within CMIP3 and AR4, revealed notable discrepancies in simulating NWPSH characteristics. Models with higher meridional resolution showed some advantages, yet substantial uncertainties persisted among different models (Huang et al., 2009). Specifically, AR4 analyses indicated weaker simulation capabilities regarding interannual variability of key meteorological elements in East Asia, with better accuracy observed in simulations of the 500-hPa geopotential height field compared to sea-level pressure and 850-hPa wind fields (Zhang, 2011).

The subsequent CMIP5 models have made significant improvements over CMIP3, particularly regarding physical process simulations. Despite notable progress, inaccuracies remain evident in simulations of the 500-hPa geopotential height field. However, CMIP5 models demonstrated stronger capabilities in representing the spatial patterns and magnitudes of geopotential height and latitudinal wind changes (Liu, 2014; Chen, 2019). Nevertheless, previous studies consistently highlight inherent inaccuracies and discrepancies between model forecasts, arising from differences in horizontal resolution and predictive effectiveness.

The sixth phase of the Coupled Model Intercomparison Project (CMIP6), initiated in 2019 by the World Climate Research Program (WCRP), includes 112 climate models from 33 global institutions. Compared to its predecessors, CMIP6 features a broader array of numerical experiments, significantly improved resolutions, and more complex physical process representations, providing critical data inputs for the IPCC Sixth Assessment Report (AR6) (Zhou, 2019; Wu, 2019). The advancements within the CMIP6 models promise to enhance global climate research substantially over the next decade (Zhou, 2014; Zhao, 2018; Chen, 2020a; Brunner et al., 2020).

Amid increasingly severe global climate challenges, the IPCC Special Report on Global Warming of 1.5°C (IPCC, 2018) has emphasized the urgency of achieving net-zero emissions by 2050. Responding proactively, China has committed internationally to carbon peaking by 2030 and carbon neutrality by 2060, heightening global interest in understanding future climate trends. The Shared Socioeconomic Pathways (SSPs) scenarios within CMIP6, ranging from sustainable development (SSP1-2.6) to fossil-fuel-intensive growth (SSP5-8.5), provide an essential framework linking socio-economic factors with future climate mitigation and adaptation measures (Norgate et al., 2024). Thus, exploring these scenarios helps achieve a multi-dimensional understanding of future climate and environmental impacts.

Although extensive studies have been conducted on the NWPSH and climate models have continually advanced in their predictive capabilities, several critical scientific questions remain unresolved, particularly regarding the latest generation of CMIP6 climate models:

1. How well do current CMIP6 coupled models simulate the spatial distribution and long-term variability of the NWPSH?
2. What are the major differences and uncertainties among the CMIP6 models in simulating the position, intensity, and area of the NWPSH?
3. How will the spatial position and intensity of the NWPSH evolve under different future emission scenarios?

http://www.aloki.hu ● ISSN 1589 1623 (Print) ● ISSN 1785 0037 (Online)
DOI: http://dx.doi.org/10.15666/aeer/2304_78997919

To address these scientific questions, this study specifically aims to: firstly, evaluate the performance of the latest CMIP6 coupled models in simulating the climatological characteristics and long-term trends of the NWPSH; secondly, investigate inter-model consistencies and uncertainties in simulation results; and finally, explore future changes in the NWPSH under multiple SSP emission scenarios, identifying models with robust simulation capabilities to provide scientific insights and guidance for future predictions and model improvements.

Materials and methods

Data

The monthly mean data of 13 typical models in CMIP6 are selected in this study (https://esgf-node.llnl.gov/projects/cmip6/) (Wang et al., 2021), and the basic information of the models is shown in *Table 1*. The ensembles' first variant label (r1i1p1f1) is selected for each model. In addition to the historical information, data on the predicted values (2015-2100) of the geopotential height under the four shared socio-economic pathways (SSP1-2.6, SSP2-4.5, SSP3-7.0, SSP5-8.5) are also included (*Table 2*). The historical simulation data from 1980 to 2015 were selected as the historical period data, and the data from 2015 to 2100 under the emission scenario were chosen as the future period data. The geopotential height field data provided by NCEP/NCAR (National Centers for Environment Prediction/National Center for Atmospheric Research) are selected as the observation data for the analysis. Due to the differences in horizontal resolution among the models, the data from each model were bilinearly interpolated in this study, resulting in a resolution of 2.5° × 2.5°for all data.

Table 1. *Main information of the 13 CMIP6 coupling models selected in this study*

Models	Organization	Country/region	Horizontal resolution (longitude grids × latitude grids)
ACCESS-CM2	CSIRO-ARCCSS-BoM	Australia	192 × 144
ACCESS-ESM1-5	CSIRO	Australia	192 × 145
BCC-ESM1	BCC	China	128 × 64
CESM2	NCAR	USA	288 × 192
NESM3	NUIST	China	192 × 96
EC-Earth3	EC-Earth-Consortium	Europe	512 × 256
EC-Earth3-Veg	EC-Earth-Consortium	Europe	512 × 256
CanESM5	CCCMA	Canada	128 × 64
MIROC6	MIROC	Japan	256 × 128
FGOALS-f3-L	LAP, CAS	China	288 × 180
FGOALS-g3	LAP, CAS	China	180 × 80
MRI-ESM2-0	MRI	Japan	320 × 160
KACE-1-0-G	NIMS	South Korea	192 × 144

Methods

Meteorologically, the range corresponding to the 5880-gpm contour in the 500-hPa geopotential height field in the Northwestern Pacific Ocean (10°-45°N, 110°-180°E) is generally used to represent WNHSP (Zhao, 1999). The following indexes are used to quantitatively characterize the location and intensity of the WNHSP and its changes (Liu et al., 2012; Wang et al., 2020).

http://www.aloki.hu ● ISSN 1589 1623 (Print) ● ISSN 1785 0037 (Online)
DOI: http://dx.doi.org/10.15666/aeer/2304_78997919

***Table 2.** Shared socio-economic pathway scenario classification and main features*

Scenario	Socio-economic pathway (SSP)	Radiative forcing	Temperature rise range	Core features
SSP1-2.6	SSP1 (sustainable development pathway)	2.6 W/m²	1.5-2.0°C	Stringent climate policies, green and low-carbon transition
SSP2-4.5	SSP2 (intermediate pathway)	4.5 W/m²	2.5-3.0°C	Medium climate policy, continuing the current historical trend, utilizing a mix of energy
SSP3-7.0	SSP3 (regional competitive pathway)	7.0 W/m²	3.5-4.5°C	Weak climate policies; high levels of development imbalances between countries
SSP5-8.5	SSP5 (fossil fuel dominated pathway)	8.5 W/m²	4.5-6.0°C	Absence of climate policies, energy-intensive development

NWPSH indexes

(1) Area index: The number of grid points with mean geopotential heights greater than 5880-gpm within the range of 110° E~180° E north of 10° N. (2) Intensity index: Cumulative difference between the geopotential height value and 5870-gpm for grid points with a mean geopotential height greater than 5880-gpm. (3) Western extensional ridge points: the longitude of the westernmost position of the 5880-gpm contour within the range of 90°E~180°E is defined as the western ridge point of the NWPSH. (4) Ridge index: On the 500-hPa geopotential height map of the 2.5° × 2.5° grid, take the 17 meridians within the range of 110~150° E (with an interval of 2.5°) and average the latitude at which the maximum point of geopotential height is located in each meridian, and the resultant value is defined as the intensity index of the NWPSH.

Taylor diagram

This study also uses the Taylor diagram method (Taylor, 2001) to compare the results from inter-models and model-observation. The Taylor diagram method is a way to centralize information related to multiple modes on the same diagram for comparison, which includes three major indicators: the standard deviation, representing the average standard deviation of the model itself in the above spatial range, used to measure the simulation of amplitude; the correlation coefficient, representing the model's correlation coefficient of the model with the observation in the same spatial domain, indicative of the model's simulation capability for climate change, and the RMSE, indicating the error between the actual and the simulation values. Through these three evaluation indexes, the simulation ability of different models can be shown more clearly on the same map, which is convenient for comparison.

The Northwestern Pacific Subtropical High performs strongest in summertime and exhibiting the most obvious morphological changes, and being closest to China in summer with most significant impact (Wu, 2003; Xiao, 2018), therefore this study focuses on the spatial distribution and long-term trend changes of The Northwestern Pacific Subtropical High in summer (JJA). The NWPSH indexes defined above can be evaluated in inter-model comparison and model-observation comparison to assess the model forecast accuracy and fitness, and to obtain the optimal model.

http://www.aloki.hu ● ISSN 1589 1623 (Print) ● ISSN 1785 0037 (Online)
DOI: http://dx.doi.org/10.15666/aeer/2304_78997919

Climatology correction

Climate model outputs often contain systematic deviations due to factors such as internal climate variability, imperfect parameterizations, insufficient spatial resolution, and uncertainties in external forcings. In particular, coupled atmosphere-ocean models may introduce spurious trends over long periods, a phenomenon known as climate drift (Chen, 1997). To address systematic biases in model simulations, a climatology correction is applied to the 500-hPa geopotential height field simulated by each CMIP6 model.

To reduce the influence of such biases while preserving the models' ability to represent temporal variability, this study adopts a climatology correction method (*Eq. 1*). The method assumes that the simulated field can be decomposed into a climatological mean and an anomaly (i.e., departure from the mean). Instead of correcting both components, only the model's climatological state is replaced with the observed climatological mean, while the model-simulated anomalies are preserved. This approach is expressed as:

$$h'_{model} = \left(h_{model} - \overline{h_{model}}\right) + \overline{h_{NCEP}} \quad \text{(Eq.1)}$$

h'_{model} is the bias-corrected geopotential height at 500-hPa used in the subsequent analysis; h_{model} is the raw simulated field at a specific grid point and time; $\overline{h_{model}}$ is the multi-year mean of the model at the same grid point; $\overline{h_{NCEP}}$ is the NCEP/NCAR reanalysis climatological mean, calculated over a long-term baseline to reflect the true climatological state.

Climatology correction method ensures that the interannual variability and temporal evolution simulated by the model are retained, while the mean state bias is adjusted using observed data. It helps reduce models' climate drift and facilitates more reliable inter-model and model-observation comparisons. This approach offers several advantages: By preserving the model's internal variability, it maintains the integrity of interannual and long-term fluctuations, which are critical for trend analysis. At the same time, it effectively eliminates systematic biases in the climatological mean without distorting the underlying physical dynamics of the model. Furthermore, the method enhances comparability both across different models and between model outputs and observational data, facilitating a more consistent and robust evaluation framework.

Despite its advantages, this method has certain limitations. Applying the same method of correction uniformly across diverse models may obscure differences arising from internal physics. structural designs. Additionally, the correction is applied only on the 500-hPa geopotential height, the geopotential biases in some key dynamical factor such as wind fields or surface pressure, which have been proved that linked to the NWPSH, are not addressed. Lastly, due to the studying region and period, using NCEP/NCAR reanalysis as the observational reference introduces its own uncertainties, especially in data-sparse sea regions.

Results

Model simulations of 500-hPa geopotential height and climatology corrections

The models selected in this study show high reliability in the simulation of the NWPSH climate state (*Fig. 1*), the correlation coefficients of all the models involved in the evaluation reach more than 0.95. As for the top 5 models (EC-Earth3, EC-Earth3-Veg, FGOALS-f3-L, CESM2, and BCC-ESM1), the correlation coefficients are all more than 0.985, the standard deviation ratios are controlled in the range of 0.95-1.08, and the TSS scores are over 0.97 (*Table 3*). The three indicators synergistically verify the model's capability of accurately capturing the spatial shape of the 500-hPa geopotential height field, the strength of variability, and the distribution of the climatic state, indicating that the CMIP6 models selected in this study have a higher credibility for the simulation of the climatic state, a stronger simulation capability, and is suitable for the subsequent. It is suitable for simulations and comparisons of the climate characteristics for NWPSH.

Comparison of model simulations of climate characteristics of NWPSH

Comparison of spatial patterns of NWPSH

In order to quantitatively describe the intensity and location of the Northwestern Pacific Subtropical High, this study uses the 500-hPa geopotential height field data of each model to analyze the intensity, location and the morphology and intensity elements of the NWPSH, which can be obtained from the 5880-gpm contour of the 500-hPa geopotential height field.

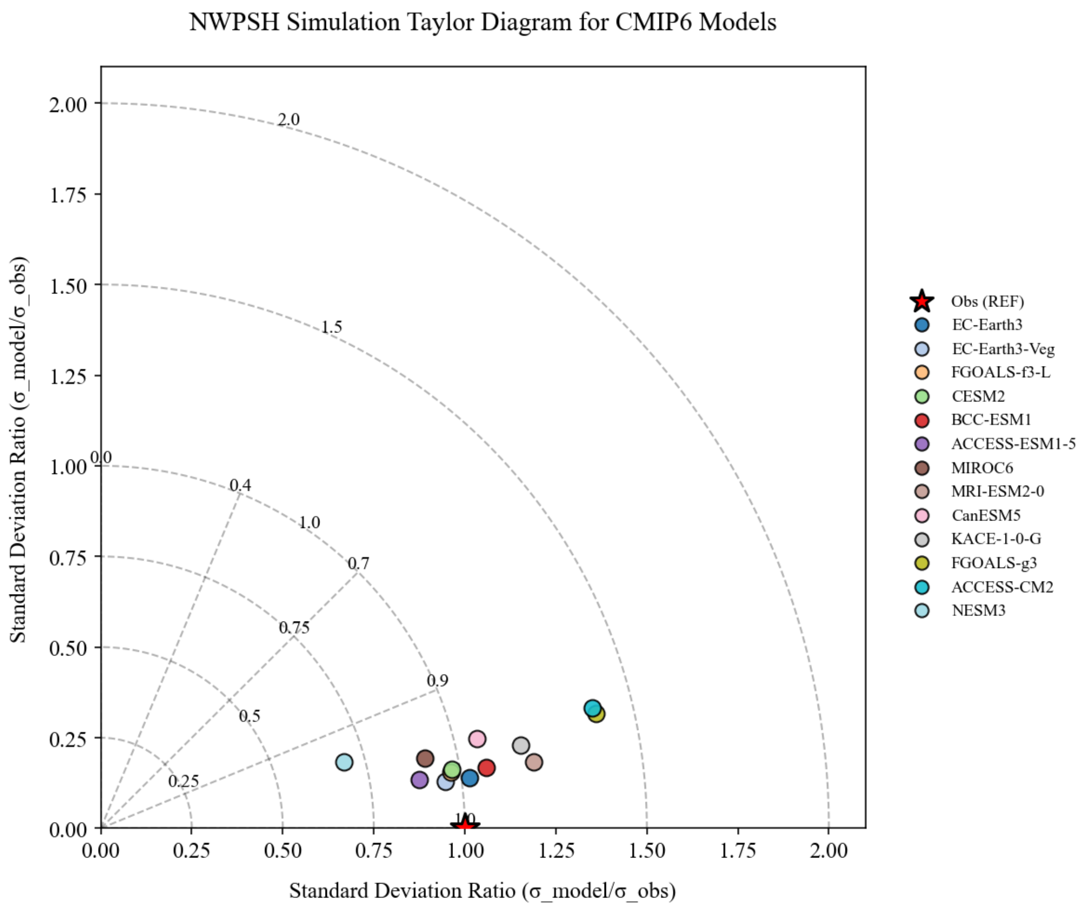

Figure 1. *Taylor diagram of the CMIP6 model with observations of the 500-hPa geopotential height field in the NWPSH region of the Northwest Pacific Ocean in summer. REF point indicates the reference of 1. The radial distance from the origin represents the normalized standard deviation ratio (model/observation). The cosine of the azimuthal angle quantifies the spatial pattern correlation coefficient, while the Euclidean distance from the REF marker corresponds to the root-mean-square error (RMSE)*

http://www.aloki.hu ● ISSN 1589 1623 (Print) ● ISSN 1785 0037 (Online)
DOI: http://dx.doi.org/10.15666/aeer/2304_78997919

***Table 3.** Ranking of CMIP6 model-simulation capability of 500-hPa geopotential height in NWPSH summertime*

Rank	Model	TSS	Correlation coefficients	Std_Ratio
1	EC-Earth3	0.980811	0.990601	1.023377
2	EC-Earth3-Veg	0.979713	0.990863	0.954372
3	FGOALS-f3-L	0.973714	0.987093	0.973154
4	CESM2	0.971840	0.985997	0.978780
5	BCC-ESM1	0.970837	0.987719	1.072985
6	ACCESS-ESM1-5	0.962692	0.988403	0.885469
7	MIROC6	0.946774	0.977214	0.910095
8	MRI-ESM2-0	0.944414	0.988388	1.202782
9	CanESM5	0.942375	0.972337	1.062212
10	KACE-1-0-G	0.937016	0.980715	1.176476
11	FGOALS-g3	0.850817	0.974046	1.396041
12	ACCESS-CM2	0.847919	0.971049	1.390240
13	NESM3	0.815731	0.964305	0.692942

In the models without correction, there are large differences between NWPSH patterns predicted by these models (*Fig. 2*), and all exhibit a significant deviation from the observation pattern. Specifically, six models including ACCESS-CM2, EC-Earth3, EC-Earth3-Veg, FGOALS-f3-L, KACE-1-0-G, and MIROC6 fail to simulate the 5880-gpm line, in contrast, the CESM2 and FGOALS-g3 models overestimate the intensity, which shows the lack of predict ability in intensity. In Conclusion, the morphology of the 5880-gpm line simulated by each model is quite different from the actual situation. Morphologically, the ACCESS-ESM1-5, BCC-ESM1, MRI-ESM-2-0, and CanESM5 models provide relatively better forecasts, and their morphologies are closer to the observations. After the climatology correction (*Fig. 3*), the simulation effect of all the models obtains a large improvement, and all of them simulate the morphology of the NWPSH and the characteristics of the western extend ridge point very well. According to the Taylor diagrams, it is found that the BCC-ESM1, ACCESS-ESM2 and EC-Earth3 models are more consistent with the observations in terms of morphology and intensity, and the western extend ridge point is the closest to the actual situation.

Northwestern Pacific Subtropical High indexes in summertime

In order to quantitatively evaluate the simulation capability of the CMIP6 models for the NWPSH, the Area index, Intensity index, Westward ridge point, and Ridge index of each model and observation are calculated and presented in the form of line graphs, so as to compare the trend and the difference between the model and the observation. In the observations, the distribution of the 5880-gpm contour ranges from 15°N to 30°N and extends westward over 140°E, which is in a more westerly and stronger circulation background compared with the multi-year average state of the NWPSH. The uncorrected model simulations are weak, and the simulated regions are also far from the real situation.

Area index

In the observation data, the area index fluctuates from 0 to 200 units throughout the years, and the unrevised area index (*Fig. 4a*) reveals that there is a large degree of bias in

http://www.aloki.hu ● ISSN 1589 1623 (Print) ● ISSN 1785 0037 (Online)
DOI: http://dx.doi.org/10.15666/aeer/2304_78997919

the data corresponding to each different year. According to the ensemble average of the data, it can be seen that except for some years, the deviation of other years is more remarkable, the CESM2, BCC-ESM1, and FGOALS-g3 models have a larger deviation from the observation. and the Area index is higher. the ACCESS-ESM1-5 and EC-Earth3 models can simulate the peak of area index in the first half of the period, after the climatology correction (*Fig. 5a*), the area index of all models is well improved, and almost all of these models demonstrate improved performance in simulating the area index. However, in the latter half of the study period, all models exhibit a positive bias relative to the actual observations, the shortcoming of the instability of the CESM2 is not solved by the correction, and the difference between the models gradually increased.

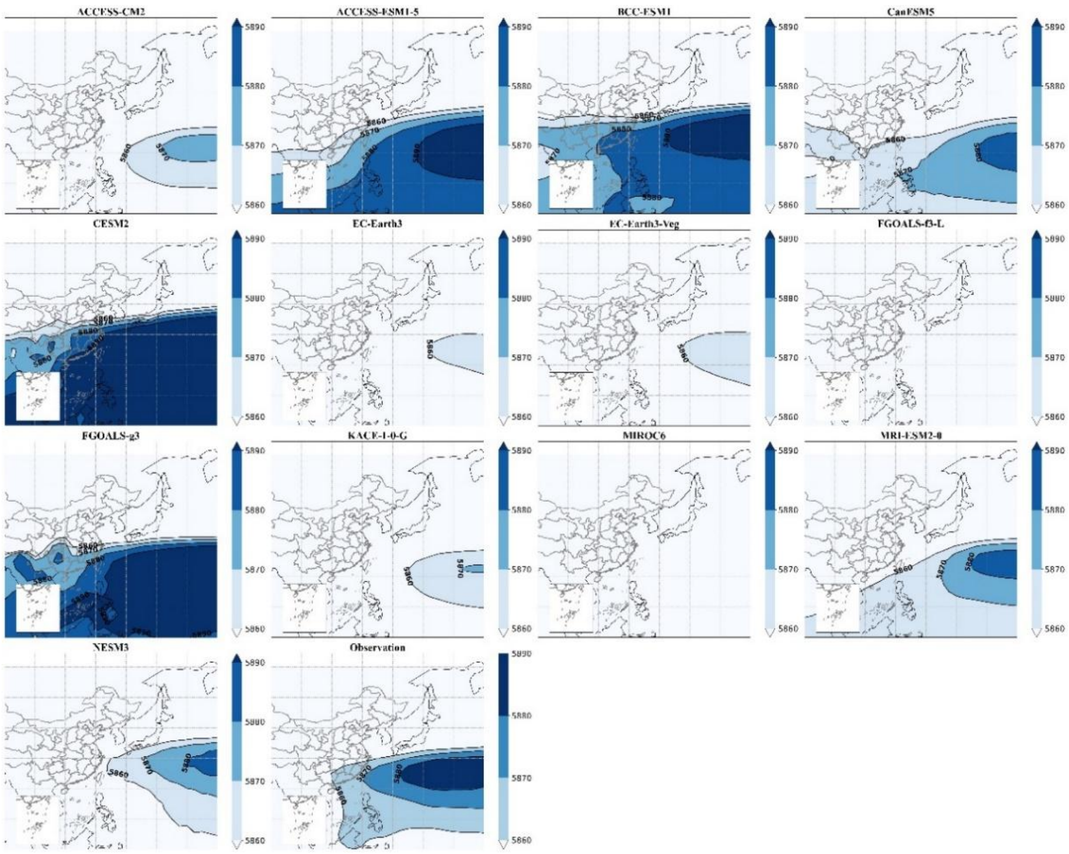

Figure 2. *Multi-year average spatial distribution of the 500-hPa geopotential height field (in gpm) for the observation and simulations of 13 CMIP6 models from 1980-2015 summertime, without the climatology correction*

Intensity index

The observed intensity index exhibits an upward trend, peaking around 2014. The fluctuation trend of the intensity index in the simulation before the correction of the climate state is relatively close to the observation, which can reflect the periodicity of the NWPSH changes. However, the bias is relatively large in terms of specific data for each year, with the BCC-ESM1, MIROC6 and CESM2 all exhibiting a positive bias and simulating a strong NWPSH, whereas the EC-Earth3 and NESM3 simulate a smaller intensity, and overall, the intensity index without the climatology correction (*Fig. 4b*) are only able to simulate a trend in the NWPSH. The intensity index model with correction

http://www.aloki.hu ● ISSN 1589 1623 (Print) ● ISSN 1785 0037 (Online)
DOI: http://dx.doi.org/10.15666/aeer/2304_78997919

is more relevant to the observations and closer to the real values in each year of the simulation, among which the CESM2 with climate state revision (*Fig. 5b*) has the largest change in the whole, and the prediction level has been greatly improved.

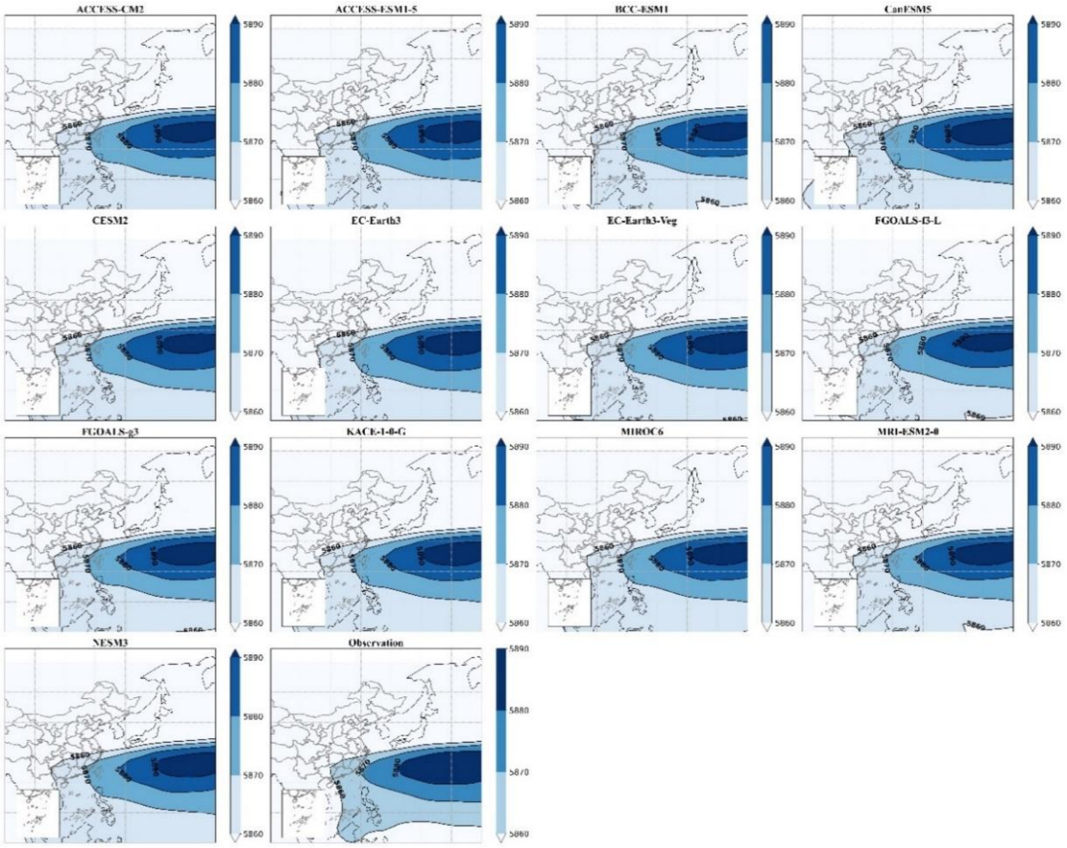

Figure 3. *Multi-year average spatial distribution of the 500-hPa geopotential height field (in gpm) for the observation and simulations of 13 CMIP6 models from 1980-2015 summertime, with the climatology correction*

As for the corrected models, in the first half of the study period, all of them are able to represent the Intensity index of the NWPSH better. However, in the latter half of the study period, the fluctuations of each model are relatively large, and the fluctuations of the CESM2 are especially obvious in the simulations in recent years, and the model simulations have a tendency to become larger. On the whole, the simulation in the EC-Earth3-Veg is more stable, and the difference between the simulated intensity of the NWPSH and the actual values is relatively small.

Western extensional ridge point

The western extensional ridge points of the Northwestern Pacific Subtropical High regularly extend westward and recedes eastward with time (Xu, 2001), in each year's observation, the Western extensional ridge points receded eastward to 170°E as its weakest point and westward to 105°E as its strongest point. Most of the models without correction can only predict the westward and eastward recession of the westward ridge point but unable to accurately represent the shape of the NWPSH in each year: the westward ridge point simulated by the CESM2 is located at 120°E, while the western

http://www.aloki.hu ● ISSN 1589 1623 (Print) ● ISSN 1785 0037 (Online)
DOI: http://dx.doi.org/10.15666/aeer/2304_78997919

extensional ridge point of the EC-Earth3 is located east of 180°E; The ACCESS-ESM1-5 simulates the Western extensional ridge point in the first half of the period, but the simulation strength decreases in the latter half of the period. After the correction, the accuracy of the model simulations is improved and closer to the actual conditions, and the EC-Earth 3 shows the most obvious improvement. All models simulate the western extensional ridge point to be westward compared with the real condition, which is consistent with the previous experimental results.

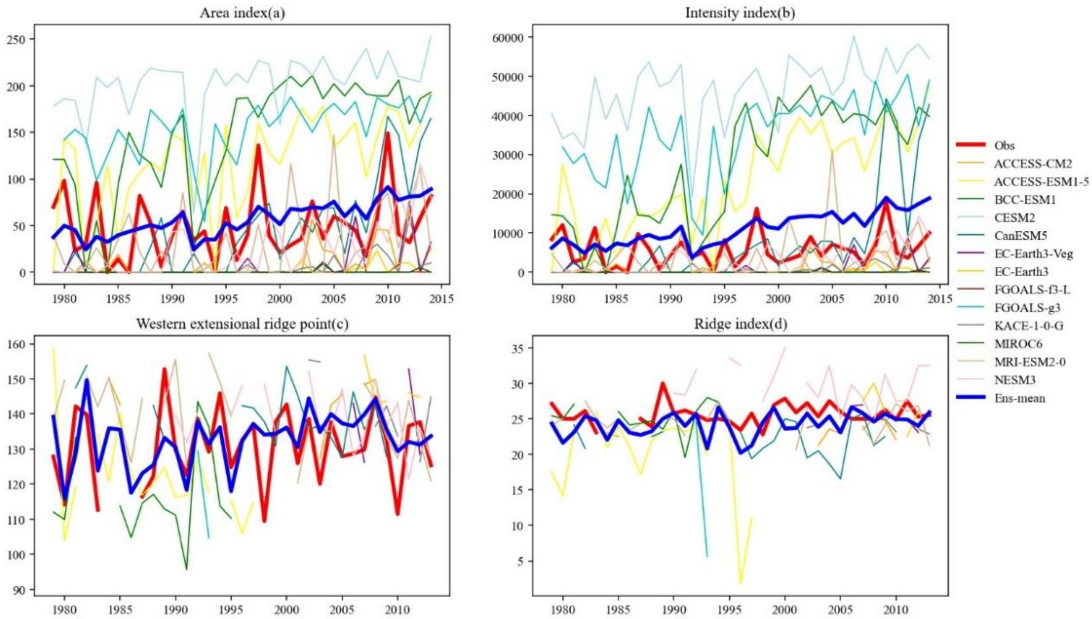

Figure 4. *NWPSH indexes for each model and observation from 1980 to 2014 summertime without the climatology correction*

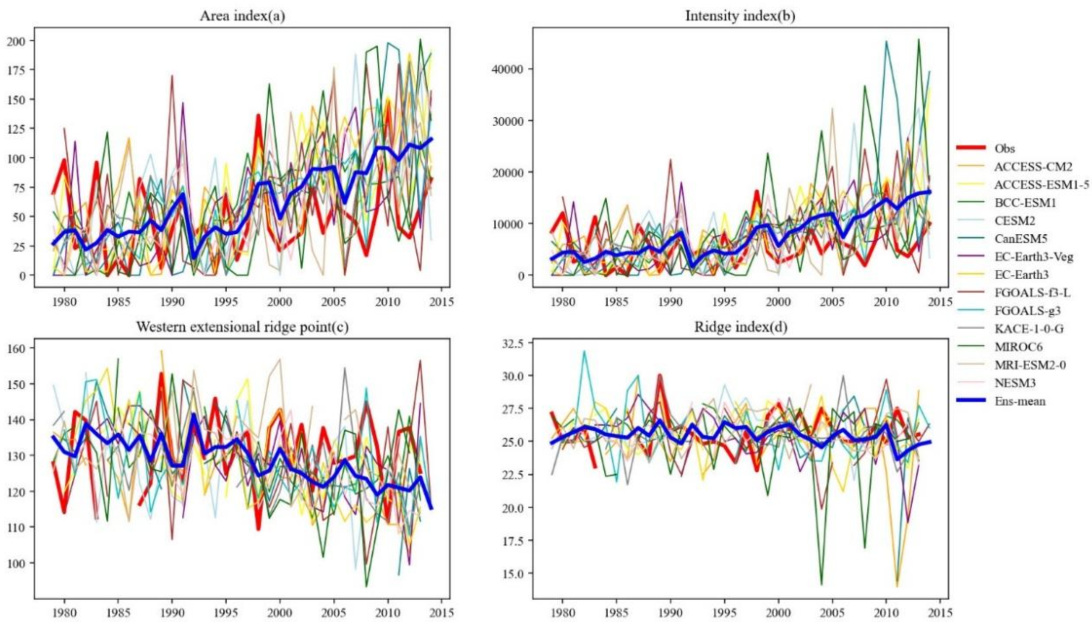

Figure 5. *NWPSH indexes for each model and observation from 1980 to 2014 summertime with the climatology correction*

http://www.aloki.hu ● ISSN 1589 1623 (Print) ● ISSN 1785 0037 (Online)
DOI: http://dx.doi.org/10.15666/aeer/2304_78997919

Ridge point

In the observation, the ridge index all fluctuated above and below 25°N, with small fluctuations and weak variations from year to year (*Figs. 4d* and *5d*), none of the models simulate the ridge index to around 30°N, and the model ensemble averages show that the average ridge index of the model forecasts is around 25°N, and the interannual variability of the ridge index is larger for each model, indicating a lack of stability in the model simulation of the ridge. The ACCESS-ESM1-5 and MIROC6 simulate the index poorly, and the EC- Earth3 simulates the index too far northerly. After the revision of the climate state, the accuracy of the model simulations has been greatly improved, with a better fit to the observation, a more significant trend, and no abrupt changes in the data of the models.

The above quantitative indexes of the NWPSH are important for understanding the simulation of the NWPSH by different models, and each parameter illustrates the simulation degree of the NWPSH by different models from different perspectives. The intensity index corresponds to the intensity of the NWPSH, and the western extensional ridge point, area index and ridge index correspond to the spatial pattern. In the simulation, it can be found that the differences between the models without climate state revision is large, and the differences between the models with the observation data is also large, so it can be said that the simulation is not effective without the revision, and after the revision of the climate state, the simulation effect of the models is effectively improved, and the simulation ability is also significantly improved. (1) There are stability differences between the models, for example, the CESM2 and MIROC6 have lower stability, and the simulations before and after the revision have distinct differences, while the ACCESS-ESM1-5, EC-Earth3-Veg and EC-Earth3 have more stable performances in the simulation. (2) There are differences in simulation accuracy between models and models, based on the simulation of the above indexes, ACCESS-ESM1-5 and EC-Earth3-Veg are more capable of capturing the trends, while in the simulation of the westward extending ridge point, MIROC6 does not reproduce the eastward retrogressing turning point after 2000 although it can reflect the long-term westward extending trend. these differences reveal that These differences reveal that the response mechanisms of different models to the internal variability and external forcing of the climate system are fundamentally different (Lin and Zeng, 1998; Zhao, 2021).

The considerable spread among the CMIP6 models in simulating the NWPSH's spatial extent, intensity, and ridge position can be largely attributed to differences in two interconnected aspects:

External forcing bias represented by the tropical sea temperature field (SST)

First of all, the spatial bias in tropical sea surface temperatures (SSTs) over the Northwestern Pacific exerts a substantial influence on regional convective heating, which is critical for the establishment, maintenance, and interdecadal variability of the NWPSH. (Takashi and Yuta, 2025; Ayugi et al., 2021) The EC-Earth3 and EC-Earth3-Veg models demonstrate notable skill in reproducing the post-1970 warming trend in the Indian Ocean and the SST anomalies during the decaying phase of ENSO. As a result, the simulated NWPSH ridgelines are more consistent with observations and exhibit a clear westward extension. In contrast, CESM2 and MIROC6 models exhibit cold biases over the equatorial western Pacific, which suppress convective heating and lead to an eastward displacement of the simulated NWPSH ridge.

http://www.aloki.hu ● ISSN 1589 1623 (Print) ● ISSN 1785 0037 (Online)
DOI: http://dx.doi.org/10.15666/aeer/2304_78997919

Internal physical structure of models

Secondly, the internal structure of the models and the treatment of key physical processes play a decisive role in simulating the configuration of the NWPSH (Dutta et al., 2022; Ruprich-Robert et al., 2021). Model resolution reflects its capability to resolve mesoscale weather systems and the boundary characteristics of the NWPSH. Higher-resolution dynamical cores (e.g., EC-Earth3, EC-Earth3-Veg and MRI-ESM2-0) better resolve monsoon trough－NWPSH interactions, whereas lower-resolution models (ACCESS-CM2, KACE-1-0-G) smooth the 5880-gpm contour, suppressing intensity peaks.

In summary, the biases in simulating the NWPSH are not only significantly influenced by differences in tropical SST distributions but are also closely linked to the internal structure of the models and the representation of physical processes. This study suggests that improving the accuracy of tropical SST simulations, along with the continued refinement of ocean-atmosphere coupling parameterizations, is essential for enhancing the reliability of NWPSH projections in future climate models (Khadka et al., 2022).

Characteristics of the linear trend of the Northwestern Pacific Subtropical High indexes

In this study, the linear trend coefficients of the NWPSH Indexes for each model are calculated to further quantitatively assess the simulation capability of the CMIP6 models (*Fig. 6*). Since the ridge index has an interannual variation cycle and the linear trend is not obvious, it is not included here. The observation shows that the linear increase of the area index from 1980 to 2014 reaches 0.958 gr/year, and the increase of the intensity index reaches 29.24 gpm/year, and each model gives the result of increasing trend in simulating the area index and intensity index, which shows that each model can show the changing trend of increasing and enhancing of the NWPSH. The western extensional ridge point shows a slow eastward trend of -0.122°/year, as most of the models also give the result of eastward shift of the WNPSH, which may be due to the thermal enhancement caused by global warming that dominates the overall strength and area enlargement of the NWPSH, and the 5880-gpm contour is misleading as an indicator of the strength of the NWPSH in the context of climate warming because its systematic elevation only reflects the global warming instead of the 5880-gpm contour is misleading as an indicator of NWPSH intensity in the context of a warming climate, as its systematic increase reflects only global warming rather than an enhancement of the itself, but rather an eastward shift of the NWPSH due to the weakening of thermal winds driven by a reduced meridional temperature gradient to the north (He and Zhou, 2015).

Standard deviation of the summer Northwestern Pacific Subtropical High indexes

The standard deviation of the NWPSH indexes is an approach to measure the amplitude of model-simulated year-to-year variability of the NWPSH index. The folded line in *Figure 7* shows the ratio of the standard deviation of the CMIP6 models in NWPSH indexes to the standard deviation of the observation, the closer the ratio is to 1, the closer the simulated year-to-year variation of the index is to the observation, and the gray bars indicate the sum of the ratio of the standard deviation of the four NWPSH indexes to the distance from the standard value of 1. The ratios of the standard deviation of the NWPSH indexes of most of the revised models are larger than 1, which indicate that the model-simulated indexes The year-to-year trend of the model simulated indexes

http://www.aloki.hu ● ISSN 1589 1623 (Print) ● ISSN 1785 0037 (Online)
DOI: http://dx.doi.org/10.15666/aeer/2304_78997919

is larger than that of the observation situation, among which the MIROC6 and the CESM2 simulate the largest variation of the NWPSH indexes. Combining the model simulations of the four indexes of the Northwestern Pacific Subtropical High, MRI-ESM2-0, EC-Earth3-Veg and ACCESS-CM2 show better simulation ability for the overall characteristics of the NWPSH in summer, which is the closest to the observations.

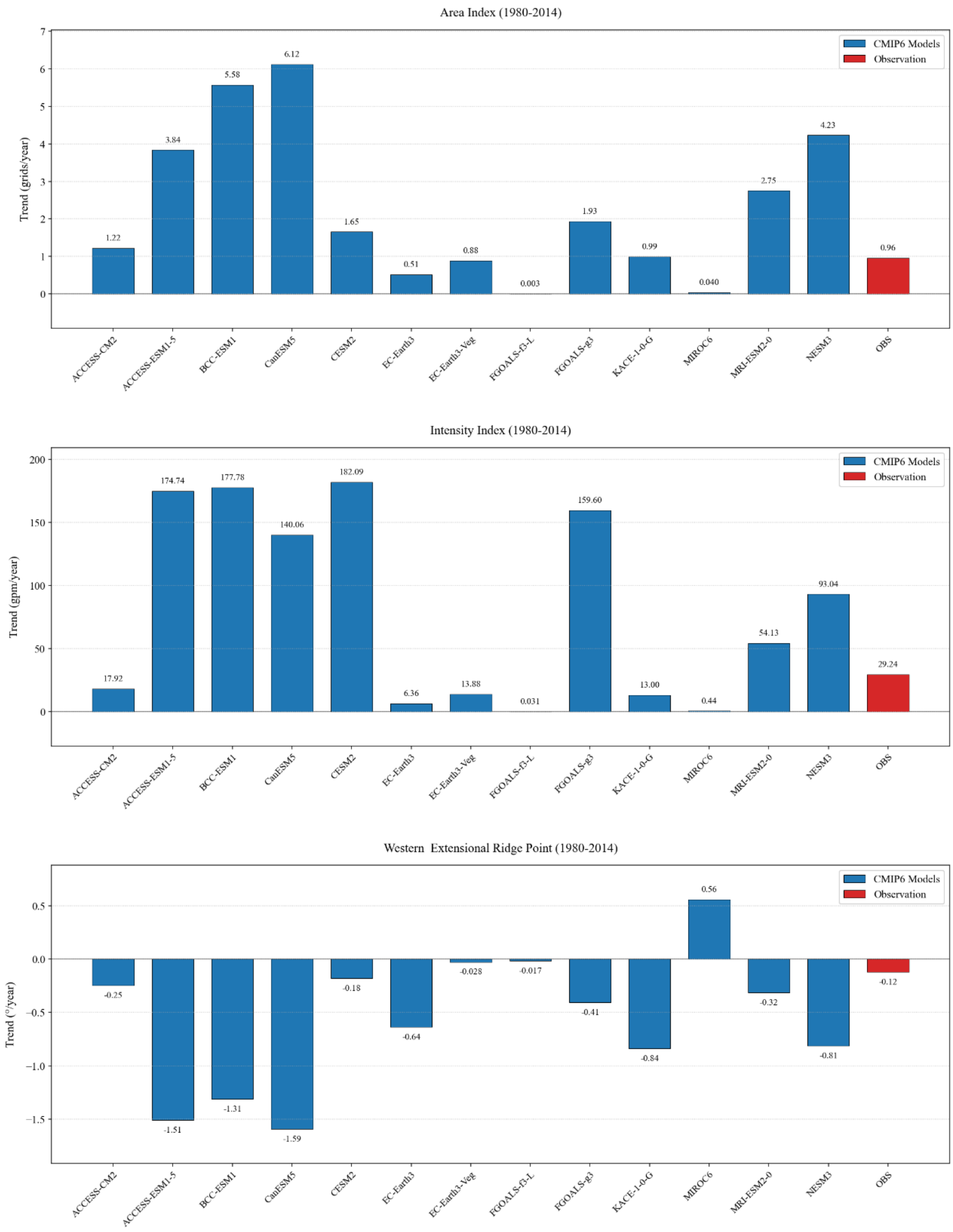

Figure 6. *1980~2014 observations (red) and CMIP6 models (blue) of the Linear trend coefficients for each NWPSH Index in summertime*

http://www.aloki.hu ● ISSN 1589 1623 (Print) ● ISSN 1785 0037 (Online)
DOI: http://dx.doi.org/10.15666/aeer/2304_78997919

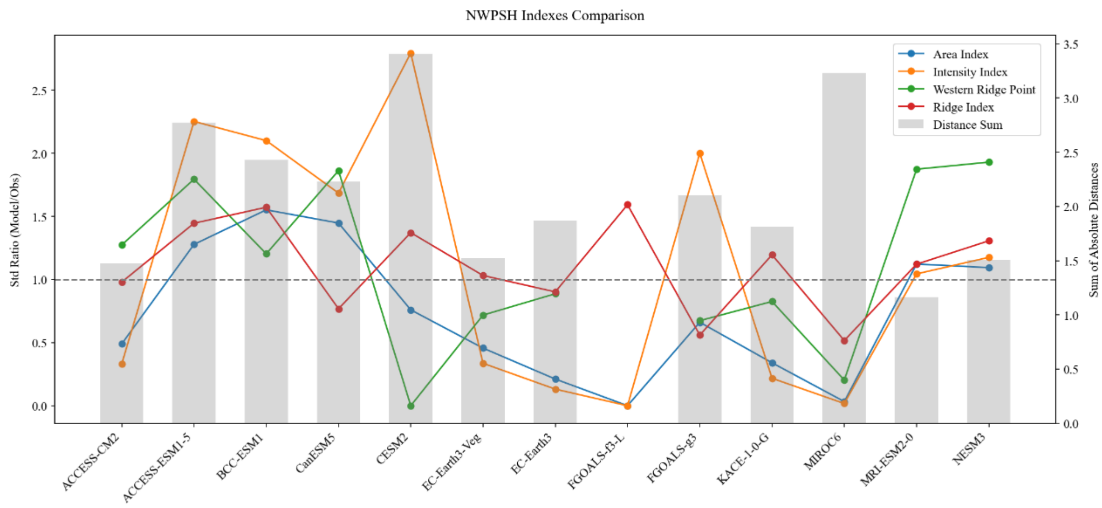

Figure 7. *Ratio of standard deviation of CMIP6 model NWPSH indexes to standard deviation of observations (gray bars indicate the distance between ratio of the standard deviations of the four indexes and the standard value)*

Possible trends of the Northwestern Pacific Subtropical High under future scenarios

In order to examine the possible trends of the 21st century NWPSH under four different shared socio-economic pathways, four indexes mentioned previously are used in this study to measure the intensity and extension of the NWPSH, and in order to take into account the model performance and simulation capability, the chosen four models that have performed relatively well in previous studies (EC-Earth, EC-Earth3-Veg, BCC-ESM1, MRI- ESM-2-0) to do the averaging, all indexes use a 9-year moving average to extract robust intergenerational change signals and eliminate the impact of short-term fluctuations.

The area index exhibits an emission-dependent growth across scenarios, with SSP5-8.5 showing the steepest increase, particularly after 2050, reaching over 400 units by 2100. SSP1-2.6 shows a more moderate trend, stabilizing after mid-century. However, the inter-model spread (±1σ) also widens substantially under higher-emission pathways, suggesting greater uncertainty in projecting the spatial expansion of the NWPSH system under intense radiative forcing.

The intensity index demonstrates similar divergence. While all scenarios project an increase from the historical mean (~25,000 gpm), SSP3-7.0 and SSP5-8.5 exhibit much sharper enhancement after the 2060s. By contrast, SSP1-2.6 shows signs of saturation, supporting the notion of a possible non-linear climate threshold (Zhou and Chen, 2015). Notably, several models deviate from the ensemble mean, indicating divergent sensitivities to upper-tropospheric temperature gradients and feedback processes.

The western ridge point exhibits the clearest structural change among the indexes, with most models under SSP5-8.5 projecting a westward retreat beyond 70°E before 2050, suggesting intensified westward extension. However, under SSP1-2.6 and SSP2-4.5, the ridge remains relatively stable or migrates only modestly. These discrepancies highlight the need to interpret long-term NWPSH shifts as scenario and model dependent rather than universal. Differences are likely related to how each model simulates western Pacific SST warming, convective heating distributions, and monsoon-subtropical interactions.

http://www.aloki.hu ● ISSN 1589 1623 (Print) ● ISSN 1785 0037 (Online)
DOI: http://dx.doi.org/10.15666/aeer/2304_78997919

The projections of the NWPSH under the four different shared socio-economic pathways all incorporate the possibility of its persistent westward extension and northward lift, which will reshape the East Asian summer wind water vapor transportation pattern under the current and higher emission background. The occurrence of regional extreme precipitation/high-temperature events will rise substantially in a high-emission context. Differences between scenarios highlight the necessity of global temperature control targets to maintain the stability of the present climate system and weather processes (He et al., 2015; He and Zhou, 2014) (*Fig. 8*).

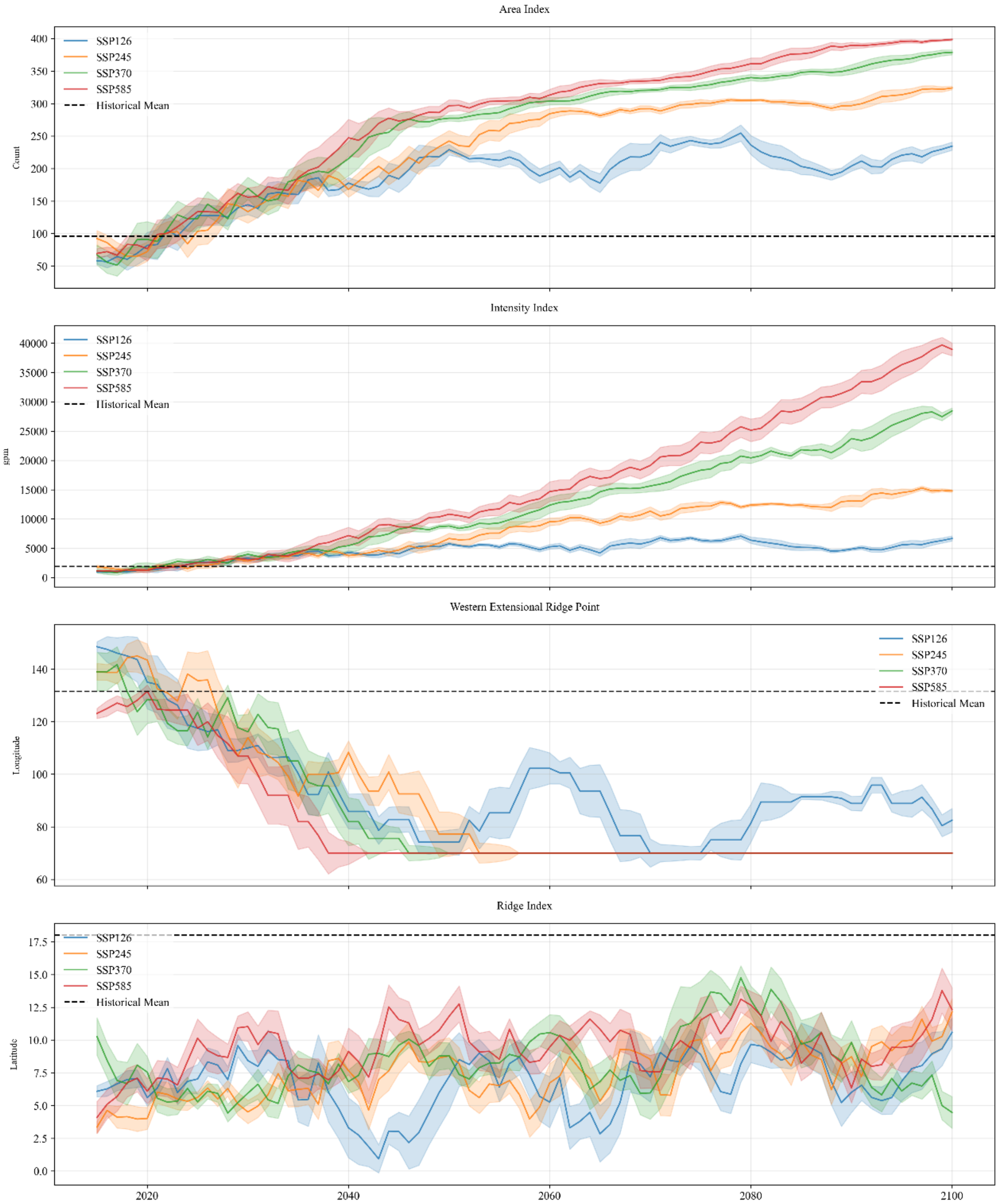

***Figure 8.** Temporal evolution of key NWPSH indexes in the CMIP6 models under various SSP scenarios (2015–2100) (shaded areas represent ± 1 standard deviation around the ensemble means)*

http://www.aloki.hu ● ISSN 1589 1623 (Print) ● ISSN 1785 0037 (Online)
DOI: http://dx.doi.org/10.15666/aeer/2304_78997919

Conclusion

This study systematically evaluates the simulation capability of thirteen CMIP6 models in representing the Northwestern Pacific Subtropical High (NWPSH), based on historical experiments and NCEP/NCAR atmospheric reanalysis data. A climatological correction method is applied to revise the mean state of model outputs, enabling more accurate assessment of the NWPSH's spatial distribution characteristics and long-term evolution. The main results are as follows:

(1) The CMIP6 models exhibit substantial systematic biases in simulating the climatological mean of the 500-hPa geopotential height and key NWPSH indexes. By applying a climatology correction using NCEP/NCAR reanalysis dataset as a reference, the models retain their intrinsic variability while reducing systematic inaccuracies. This method improves the physical reliability of the simulated NWPSH fields and provides a more consistent basis for inter-model comparisons.

(2) The simulation performance varies across models and indexes. For example, the MRI-ESM2-0 and ACCESS-ESM1-5 models demonstrate higher accuracy in capturing the spatial morphology of the NWPSH, while BCC-ESM1 performs better in reproducing the NWPSH intensity index. In contrast, CESM2 shows limitations in simulating multiple NWPSH characteristics. The results emphasize the importance of model selection and type-specific assessment in regional climate research.

(3) After climatology correction, most models reproduce the observed strengthening and expansion of the NWPSH since the 1970s more realistically. Nonetheless, consistent with prior studies (Zheng, 2021; Duan, 2011), many models still struggle to replicate the full spatiotemporal evolution of the NWPSH, particularly the ridge position and intra-seasonal variations. Through multi-index assessment, EC-Earth3, EC-Earth3-Veg, BCC-ESM1, and MRI-ESM2-0 are identified as having relatively stronger simulation capabilities, whereas CESM2 and several others exhibit persistent deficiencies. The comprehensive evaluation framework proposed here offers a robust methodology for assessing model fidelity in simulating large-scale circulation systems.

(4) Future NWPSH projections under four SSP scenarios (SSP1-2.6 to SSP5-8.5) reveal notable inter-decadal variability and scenario-dependent responses. All indexes tend to increase with greenhouse gas emissions, with the most pronounced linear trends under the SSP5-8.5 scenario and the weakest trends under SSP1-2.6.

The main contribution of this study lies in the construction of an integrated framework combining "multi-indexes assessment, climatology correction method, and future scenario comparison," which effectively quantifies model capability and simulation uncertainty, providing a more reliable scientific basis for explaining the long-term evolution of NWPSH under different emission pathways. The study provides a theoretical foundation for the selection and adaptation of climate models in regional climate prediction and risk assessment in East Asia, while also emphasizing the importance of correcting model system biases. Future research should further introduce multivariate dynamic consistency correction methods to systematically explore the coupling mechanisms between SST anomalies, convective heating, and NWPSH, thereby enhancing the robustness and operational feasibility of future regional climate predictions.

Limitation and future direction

This study provides a systematic evaluation of the NWPSH using outputs from 13 CMIP6 climate models. However, several limitations must be acknowledged:

http://www.aloki.hu ● ISSN 1589 1623 (Print) ● ISSN 1785 0037 (Online)
DOI: http://dx.doi.org/10.15666/aeer/2304_78997919

(1) Limitations of mode and scenario selection

The analysis is restricted to a subset of 13 CMIP6 models that provide complete outputs for both the historical period (1850–2014) and SSP scenarios. As such, the findings may not fully capture the broader diversity and uncertainty range of the entire CMIP6 ensemble. The analysis of future NWPSH changes is only based on the scenarios from SSP1-2.6 to SSP5-8.5, and the discussion on scenario sensitivity and the structure of socioeconomic assumptions remains insufficient (Karmouche et al., 2023).

(2) Reliance on a single reanalysis dataset

The climatology correction in this study uses NCEP/NCAR Reanalysis dataset as the single observational reference. While this dataset provides long-term continuity, it may contain biases over data-sparse regions such as tropical oceans, highlighting the potential value of multi-reanalysis approaches in future studies.

(3) A relatively basic structure of the climatology correction scheme

The climatology correction scheme employed in this study is based on a linear replacement of the geopotential height field. While the approach is straightforward and facilitates batch application across multiple models, the physical consistency and comparability of the resulting anomaly fields among models require further discussion. What is more, this scheme may exhibit limited applicability without considering the structural differences when applied to models. Additionally, the method is not able to include synchronous corrections for other dynamically related variables (e.g., wind fields, sea level pressure) (Gusain et al., 2020), which may constrain the subsequent comprehensive analysis of the dynamic structure of the NWPSH

The future work will aim at the limitation above, introducing multi-source reanalysis data for climatology correction and optimizing the structure of the method, while expanding the range of correction variables to more comprehensively improve the accuracy and physical consistency of NWPSH.

Discussion

The intensity and spatial distribution of the Northwestern Pacific Subtropical High are influenced by the thermal conditions of the underlying surface, which are significantly correlated with the pre-ENSO. If El Niño occurs in the Pacific Ocean in the winter of the previous year, the NWPSH will extend westward in the summer of the following year. Sea surface temperature anomalies in the tropical Pacific and Indian Oceans have a great influence on the NWPSH, and the warm underlying surface enables the maintenance of the 500-hPa NWPSH system (Nitta, 1987; Huang et al., 1994; Dong et al., 2017). In previous studies, the enhanced westward extension of the NWPSH in the late 1970s was due to the warming of the tropical Indian Ocean and the western Pacific Ocean (Cao et al., 2009; Chen et al., 2020b; Zhao et al., 2024), and the effect of SST on the simulation capability of the NWPSH system was not discussed in the present study, which is worthy of further study.

In this study, the CMIP6 model significantly overestimates the NWPSH, which is not only related to the model itself, but also related to the fact that most of the integrated processing schemes use algorithms focusing on a single performance or cost function, and pay less attention to the physical processes or forcing between the geophysical

http://www.aloki.hu ● ISSN 1589 1623 (Print) ● ISSN 1785 0037 (Online)
DOI: http://dx.doi.org/10.15666/aeer/2304_78997919

variables. Sun et al. (2023) utilize the idea of Pareto-optimality to constrain the simulation of the NWPSH by using the three critical zones of sea surface temperature, and further constrain it based on the constraint of "closest to the observation". The results demonstrate that the two multivariate optimization ensemble schemes reduce the simulation deviation of the NWPSH by 56% and 75%, respectively. The optimization performance is higher than that of the traditional rank-weighted scheme.

In the context of global warming generated by greenhouse gas emissions (Yang et al., 2022), the uncertainty in the NWPSH prediction mainly stems from the systematic bias of the models in the simulation of historical sea surface temperatures (SSTs). Based on the Emergent Constraint idea, after the bias revision of the models using the observed sea surface temperature, more models give enhanced results of the NWPSH under the high-emission scenario of RCP8.5, which reduces the pre-existing prediction uncertainty by 45% (Wang et al., 2017; Chen, 2020c; Zhou et al., 2024), which is important for China's future timing of major rainy seasons and forecasts of droughts and floods, as well as monsoon climate changes in East Asia, which need to be further discussed.

Acknowledgments. The research was supported by "the Fundamental Research Funds for the Central Universities" (24CAFUC03033).

REFERENCES

[1] Ayugi, B., Jiang, Z. H., Zhu, H. H., Ngoma, H., Babaousmail, H., Rizwan, K., Dike, V. (2021): Comparison of CMIP6 and CMIP5 models in simulating mean and extreme precipitation over East Africa. – International Journal of Climatology 41(15): 6474-6496.

[2] Brunner, L., Pendergrass, A. G., Lehner, F., Lorenz, R., Knutti, R. (2020): Reduced global warming from CMIP6 projections when weighting models by performance and independence. – Earth System Dynamics Discussions 2020: 1-23.

[3] Cao, J., You, Y., Huang, W. (2009): Relationship between the interannual variation of Western Pacific Subtropical High ridge surface in summer and the sea surface temperature of Pacific. – Plateau Meteorology 28(2): 411-418.

[4] Capotondi, A., McGregor, S., McPhaden, M. J., Newman, M., Deser, C., Timmermann, A. (2023): Mechanisms of tropical Pacific decadal variability. – Nature Reviews Earth & Environment 4(11): 754-769.

[5] Chang, C. P., Zhang, Y., Li, T. (2000): Interannual and interdecadal variations of the East Asian summer monsoon and tropical Pacific SSTs. Part I: Roles of the subtropical ridge. – Journal of Climate 13(24): 4310-4325.

[6] Chen, H. (2019): Simulation and projection of the Pacific Decadal Oscillation based on CMIP5 coupled models. – Chinese Journal of Atmospheric Sciences 43(4): 783-795.

[7] Chen, H. P., Sun, J. Q., Lin, W. Q., Xu, H. W. (2020b): Comparison of CMIP6 and CMIP5 models in simulating climate extremes. – Science Bulletin 65(17): 1415-1418.

[8] Chen, K. M., Jin, X. Z., Zhang, X. H. (1997): A discussion on the climate drift and sensitivity of the coupled sea-air model. – Acta Oceanologica Sinica 2: 39-46 + 51-52 (in Chinese).

[9] Chen, S. Q., Xu, F., Li, Y. J., Du, J. M., Tu, S. F., Ji, Q. Q., Yang, J. Y., Zhang, S. J., Zhang, Y., Zhi, S. Q. (2020a): Summer SST in the Northwest Pacific Ocean in the last 70 years and its correlation with the variation of the western Pacific subtropical high. – Journal of Tropical Meteorology 36(6): 846-854.

[10] Chen, X. L., Zhou, T. J., Wu, P. L., Guo, Z., Wang, M. H. (2020c): Emergent constraints on future projections of the western North Pacific Subtropical High. – Nature Communications 11(1): 2802.

http://www.aloki.hu ● ISSN 1589 1623 (Print) ● ISSN 1785 0037 (Online)
DOI: http://dx.doi.org/10.15666/aeer/2304_78997919

[11] Dong, X., Fan, F. X., Lin, R. P., Jin, J. B., Lian, R. X. (2017): Simulation of the western North Pacific subtropical high in El Niño decaying summers by CMIP5 AGCMs. – Atmospheric and Oceanic Science Letters 10(2): 146-155.
[12] Duan, M. K., Wang, P. X., Wu, H. B. (2011): The verification of NCEP ensemble probabilistic forecasts on the extreme weather events of 500 hPa geopotential heights. – Transactions of Atmospheric Sciences 34(6): 717-724.
[13] Dutta, U., Hazra, A., Chaudhari, H. S., Barman, N. (2022): Unraveling the global teleconnections of Indian summer monsoon clouds: expedition from CMIP5 to CMIP6. – Global and Planetary Change 215: 103873.
[14] Guan, W. N., Hu, H. B., Ren, X. J., Yang, X. Q. (2019): Subseasonal zonal variability of the western Pacific subtropical high in summer: climate impacts and underlying mechanisms. – Climate Dynamics 53(5): 3325-3344.
[15] Gusain, A., Ghosh, S., Karmakar, S. (2020): Added value of CMIP6 over CMIP5 models in simulating Indian summer monsoon rainfall. – Atmospheric Research 232: 104680.
[16] He, C., Zhou, T. J. (2015): Responses of the western North Pacific subtropical high to global warming under RCP4.5 and RCP8.5 scenarios projected by 33 CMIP5 models: the dominance of tropical Indian Ocean–tropical western Pacific SST gradient. – Journal of Climate 28(1): 365-380.
[17] He, C., Zhou, W. (2020): Different enhancement of the East Asian summer monsoon under global warming and interglacial epochs simulated by CMIP6 models: role of the subtropical high. – Journal of Climate 33(22): 9721-9733.
[18] He, C., Zhou, T. J., Lin, A. L., Wu, B., Gu, D. J., Li, C. H., Zheng, B. (2015): Enhanced or weakened western North Pacific subtropical high under global warming? – Scientific Reports 5(1): 16771.
[19] Hu, S., Wu, B., Wang, Y. M., Zhou, T. J., Yu, Y. Q., He, B., Lin, P. F., Bao, Q., Liu, H. L., Chen, K. J., Zhao, S. W. (2023): CAS FGOALS-f3-L model datasets for CMIP6 DCPP experiment. – Advances in Atmospheric Sciences 40(10): 1911-1922.
[20] Huang, G., Qu, X. (2009): Meridional location of West Pacific subtropical high in summer in IPCC AR4 simulation. – Transactions of Atmospheric Sciences 32: 351-359.
[21] Huang, R. H., Cai, R. S., Chen, J. L., Zhou, L. T. (2006): Interdecadal variations of drought and flooding disasters in China and their association with the East Asian climate system. – Chinese Journal of Atmospheric Sciences 30(5): 730-743 (in Chinese.
[22] IPCC (2018): Global Warming of 1.5°C: An IPCC Special Report on Impacts of Global Warming of 1.5°C Above Pre-Industrial Levels and Related Global Greenhouse Gas Emission Pathways, in the Context of Strengthening the Global Response to the Threat of Climate Change, Sustainable Development, and Efforts to Eradicate Poverty. – IPCC, Geneva.
[23] Karmouche, S., Galytska, E., Runge, J., Kretschmer, M., Schütte, S., Kruschke, T. (2023): Regime-oriented causal model evaluation of Atlantic–Pacific teleconnections in CMIP6. – Earth System Dynamics 14(2): 309-344.
[24] Khadka, D., Babel, M. S., Abatan, A. A., Pandey, V. P., Koirala, S. (2022): An evaluation of CMIP5 and CMIP6 climate models in simulating summer rainfall in the Southeast Asian monsoon domain. – International Journal of Climatology 42(2): 1181-1202.
[25] Li, X. Y., Lu, R. Y., Li, G. (2021): Different configurations of interannual variability of the western North Pacific subtropical high and East Asian westerly jet in summer. – Advances in Atmospheric Sciences 38(6): 931-942.
[26] Liu, Y. Y., Li, W. J., Ai, W. X., Li, Q. Q. (2012): Reconstruction and application of the monthly western Pacific subtropical high indices. – Applied Meteorological Science 23(4): 414-423.
[27] Liu, Y. Y., Li, W. J., Zuo, J. Q., Hu, Z. Z. (2014): Simulation and projection of the western Pacific subtropical high in CMIP5 models. – Journal of Meteorological Research 28(3): 327-340.

http://www.aloki.hu ● ISSN 1589 1623 (Print) ● ISSN 1785 0037 (Online)
DOI: http://dx.doi.org/10.15666/aeer/2304_78997919

[28] Nitta, T. (1987): Convective activities in the tropical western Pacific and their impact on the Northern Hemisphere summer circulation. – Journal of the Meteorological Society of Japan. Ser. II 65(3): 373-390.
[29] Norgate, M., Tiwari, P. R., Das, S., Prasanna, V., Kumar, B. P. (2024): On the present and future changes in Indian summer monsoon precipitation characteristics under different SSP scenarios from CMIP6 models. – Climate Dynamics 62(12): 10445-10464.
[30] Peng, J. B. (2014): An investigation of the formation of the heat wave in southern China in summer 2013 and the relevant abnormal subtropical high activities. – Atmospheric and Oceanic Science Letters 7(4): 286-290.
[31] Ruprich-Robert, Y., Moreno-Chamarro, E., Levine, X., Ortega, P., Delworth, T. L., Msadek, R., Cassou, C. (2021): Impacts of Atlantic multidecadal variability on the tropical Pacific: a multi-model study. – NPJ Climate and Atmospheric Science 4: 33.
[32] Sun, C. X., Jiang, Z. H., Tang, Z. F., Li, L. (2023): Multi-objective ensemble-processing strategies to optimize the simulation of the western North Pacific subtropical high in boreal summer. – Geophysical Research Letters 50(23).
[33] Sun, Y., Li, L. Z. X., Ramstein, G., Zhou, T. J., Tan, N., Kageyama, M., Wang, S. Y. (2019): Regional meridional cells governing the interannual variability of the Hadley circulation in boreal winter. – Climate Dynamics 52(7): 831-853.
[34] Takashi, M., Yuta, A. (2025): Decadal modulation of summertime Northwestern Pacific Subtropical High linked to Indian Ocean basin warming. – Climate 13(6): 106.
[35] Tao, S. Y. (1987): A review of recent research on the East Asian summer monsoon in China. – Monsoon Meteorology 60-92.
[36] Tao, S. Y., Wei, J. (2006): The westward, northward advance of the subtropical high over the West Pacific in summer. – Journal of Applied Meteorology and Climatology 45(5): 513-525.
[37] Taylor, K. E. (2001): Summarizing multiple aspects of model performance in a single diagram. – Journal of Geophysical Research: Atmospheres 106(D7): 7183-7192.
[38] Wang, J. Y., Wu, Z. W. (2024): Three types of East Asian summer rainfall associated with monsoon circulation and tropical cyclone activities: unique features and major influential factors. – Climate Dynamics 62(5): 4099-4116.
[39] Wang, Q. W., Hu, S. J., Jia, B., Zhou, B. Q., Gao, C. B. (2020): A new definition of the western Pacific subtropical high indexes based on three-pattern decomposition of global atmospheric circulation. – Climatic and Environmental Research 25(6): 625-636 (in Chinese).
[40] Wang, X. X., Jiang, D. B., Lang, X. M. (2017): Future extreme climate changes linked to global warming intensity. – Science Bulletin 62(24): 1673-1680.
[41] Wang, Y., Li, H. X., Wang, H. J., Sun, B., Chen, H. P. (2021): Evaluation of CMIP6 model simulations of extreme precipitation in China and comparison with CMIP5. – Acta Meteorologica Sinica 79(3): 369-386.
[42] Wu, B., Xin, X. G. (2019): Short commentary on CMIP6 Decadal Climate Prediction Project (DCPP). – Climate Change Research 15(5): 476-480.
[43] Wu, G. X., Chou, J. F., Liu, Y. M., Zhang, Q. Y., Sun, S. Q. (2002): Relation between the zonal mean subtropical anticyclone and the sinking arm of the Hadley cell. – Acta Meteorologica Sinica 60(5): 635-636.
[44] Wu, G., Chou, J., Liu, Y. (2003): Review and prospect of the study on the subtropical anticyclone. – Chinese Journal of Atmospheric Sciences 27(4): 503-517 (in Chinese.
[45] Xiao, Y. L., Chi, Z. X., Yang, D. D., Chen, Y., Kong, D. X. (2018): The characteristics of summer precipitation in eastern China and its relationship with the WPSH. – Journal of Mountain Meteorology 42(3): 44-50 (in Chinese).
[46] Xu, H. M., He, J. H., Zhou, B. (2001): The features of atmospheric circulation during Meiyu onset and possible mechanisms for westward extension (northward shift) of Pacific Subtropical High. – Journal of Applied Meteorological Science 12(2): 150-158.

http://www.aloki.hu ● ISSN 1589 1623 (Print) ● ISSN 1785 0037 (Online)
DOI: http://dx.doi.org/10.15666/aeer/2304_78997919

[47] Yang, J., Gong, D. Y., Wang, W. S., Hu, M., Mao, R. (2012): Extreme drought event of 2009/2010 over southwestern China. – Meteorology and Atmospheric Physics 115(3): 173-184.
[48] Yang, K., Cai, W. J., Huang, G., Hu, K. M., Ng, B., Wang, G. J. (2022): Increased variability of the western Pacific subtropical high under greenhouse warming. – Proceedings of the National Academy of Sciences 119(23).
[49] Yang, K., Ma, J., Chen, X. L., Wang, L. (2025): The source of the uncertainties in CMIP6 model's projections of the summertime northwest Pacific subtropical high. – Journal of Geophysical Research: Atmospheres 130(1): e2024JD040123.
[50] Zhang, H. F., Chen, H. S. (2011): Evaluation of summer circulation simulation over East Asia by 21 climate models II: interannual variability. – Scientia Meteorologica Sinica 31: 247-257.
[51] Zhao, J. Z., He, S. P., Fan, K., Wang, H. J., Li, F. (2024): Projecting wintertime newly formed Arctic Sea ice through weighting CMIP6 model performance and independence. – Advances in Atmospheric Sciences 41(1): 1-18.
[52] Zhao, Z. C., Luo, Y., Huang, J. B. (2018): The detection of the CMIP5 climate model to see the development of CMIP6 earth system models. – Climate Change Research 14(6): 643-648.
[53] Zheng, J. W., Cai, H. K., Wu, J., Heng, Z. W., Lin, Z. (2021): Performance of seasonal prediction of 500 hPa geopotential height with three operational climate prediction models. – Plateau and Mountain Meteorology Research 41(2): 115-124.
[54] Zhou, P. Y., Jiang, Z. H., Li, T. (2024): Climate projection over China under global warming of 1.5 and 2°C considering model performance and independence. – Transactions of Atmospheric Sciences 47(3): 376-391.
[55] Zhou, T. J., Chen, X. L. (2015): The uncertainty in the 2°C warming threshold issue as related to climate sensitivity and climate feedback. – Acta Meteorologica Sinica 73(4): 624-634.
[56] Zhou, T. J., Yu, R. C. (2005): Atmospheric water vapor transport associated with typical anomalous summer rainfall patterns in China. – Journal of Geophysical Research: Atmospheres 110(D8): D08104.
[57] Zhou, T. J., Zou, L. W., Chen, X. L. (2019): Commentary on the coupled model intercomparison project phase 6 (CMIP6). – Advances in Climate Change Research 15(5): 445-456.
[58] Zhou, T. J., Zou, L. W., Wu, B., Jin, C. X., Song, F. F., Chen, X. L., Zhang, L. X. (2014): Development of earth/climate system models in China: a review from the Coupled Model Intercomparison Project perspective. – Journal of Meteorological Research 28(5): 762-779.
[59] Zou, M., Qiao, S. B., Wu, Y. P., Feng, G. L. (2017): Effects of anomalous water vapor transport from tropical Indian Ocean-Western Pacific on summer rainfall in eastern China. – Chinese Journal of Atmospheric Sciences 41(5): 988-997.

http://www.aloki.hu ● ISSN 1589 1623 (Print) ● ISSN 1785 0037 (Online)
DOI: http://dx.doi.org/10.15666/aeer/2304_78997919